43

NASA CR-121220
REPORT MDC J5961

THE RESULTS OF A LOW-SPEED WIND TUNNEL TEST TO INVESTIGATE THE EFFECTS OF INSTALLING REFAN JT8D ENGINES ON THE MCDONNELL DOUGLAS DC-9-30

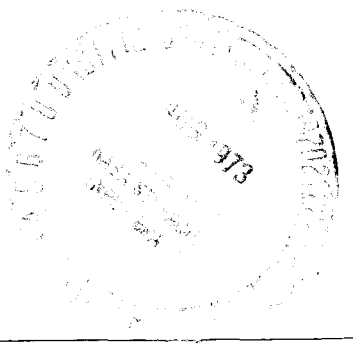

prepared for
NATIONAL AERONAUTICS AND SPACE ADMINISTRATION
NASA Lewis Research Center
Contract NAS 3-16814

DOUGLAS AIRCRAFT COMPANY
MCDONNELL DOUGLAS CORPORATION

NASA CR-121220
REPORT MDC J5961

THE RESULTS OF A LOW-SPEED WIND TUNNEL TEST TO INVESTIGATE THE EFFECTS OF INSTALLING REFAN JT8D ENGINES ON THE MCDONNELL DOUGLAS DC-9-30

prepared for
NATIONAL AERONAUTICS AND SPACE ADMINISTRATION
NASA Lewis Research Center
Contract NAS 3-16814

1. Report No.	2. Government Accession No.	3. Recipient's Catalog No.
4. Title and Subtitle The Results of a Low-Speed Wind Tunnel Test to Investigate the Effects of Installing Refan JT8D Engines on the McDonnell Douglas DC-9-30		5. Report Date June 1973 6. Performing Organization Code
7. Author(s) H. E. Chrisenberry, P. G. Doss, A. E. Kressly, R. D. Prichard, and C. S. Thorndike		8. Performing Organization Report No. MDC J5961 10. Work Unit No.
9. Performing Organization Name and Address Douglas Aircraft Company Long Beach, California		11. Contract or Grant No. NAS 3-16814 13. Type of Report and Period Covered Contractor Report
12. Sponsoring Agency Name and Address National Aeronautics and Space Administration Washington, D.C. 20546		14. Sponsoring Agency Code

15. Supplementary Notes

Project Manager, Arthur Medierous
Research Center, Cleveland, Ohio NASA/Lewis

16. Abstract

A low speed wind tunnel test was conducted in the NASA ARC 12-foot wind tunnel during February 1973 to assess the effects of the larger JT8D refan nacelles on the stability and control characteristics of the DC-9-30, with emphasis on the deep stall regime. Deep stall pitching moment and elevator hinge moment data, and low angle of attack tail-on and tail-off pitching moment data are presented. The refan nacelle was tested in conjunction with various pylons of reduced span relative to the production DC-9-30 pylon. Also, a horizontal tail that was larger than the production tail was tested. The data show that the refan installation has a small detrimental effect on the DC-9-30 deep stall recovery capability, that recovery characteristics are essentially independent of pylon span, and that the larger horizontal tail significantly increases recovery margins. The deep stall characteristics with the refan installation, within the range of pylon spans tested, are acceptable with no additional design changes anticipated.

17. Key Words (Suggested by Author(s))	18. Distribution Statement
DC-9 refanned nacelle stability and control deep stall	

19. Security Classif. (of this report)	20. Security Classif. (of this page)	21. No. of Pages	22. Price*
Unclassified	Unclassified	45	4.25

* For sale by the National Technical Information Service, Springfield, Virginia 22151

FOREWORD

The low-speed wind tunnel test described in this report was performed by the Douglas Aircraft Company, Stability and Control Branch - Aerodynamics of the McDonnell Douglas Corporation. The work sponsored by NASA Lewis and reported herein was performed between February and June 1973.

This report has been reviewed and is approved by:

John R Donelson — Date 6-27-73

J. E. Donelson
NASA Refan Project Aerodynamicist

A E Kressly — Date 6-27-73

A. E. Kressly, Acting Chief
Stability and Control Branch
Aerodynamics

R. B. Harris — Date 6-27-73

R. B. Harris
Chief Aerodynamics
Engineer for Design

O. R. Dunn — Date 6/27/73

O. R. Dunn
Director of Aerodynamics

TABLE OF CONTENTS

1.0 SUMMARY

A low speed wind tunnel test was conducted in the NASA ARC 12-foot wind tunnel in support of the NASA Refan Program. The purpose of this test was to assess the effects of the larger refan nacelle on the stability and control characteristics of the DC-9-30, with emphasis on the deep stall regime. The test was prompted primarily by the fact that the diameter of the refan nacelle is approximately 22 percent larger than that of the current production nacelle and, if the current pylons were used, the increased overall-span of the nacelle-pylons could decrease deep stall recovery capability. Previous DC-9 wind tunnel tests have shown that the nacelles and pylons have a major impact on deep stall characteristics. In anticipation of a problem with the new nacelle, two possible solutions were investigated during this test: (1) use of a smaller pylon span to minimize the overall nacelle-pylon span, (2) use of a new horizontal tail with increased span. The test was conducted in a manner that would allow the individual effects of the refan nacelle, the pylon span, and the horizontal tail size to be determined.

Analysis of the results of the test leads to the following conclusions:

1. The refan installation has a small effect on the DC-9-30 deep stall recovery capability, reducing the recovery margin by approximately 0.015 to 0.037 in pitching moment coefficient, depending on flap and slat position and pylon span. Deep stall characteristics with the refan installation and any pylon span within the range tested are acceptable with no additional design changes anticipated.

2. The effect of pylon span on deep stall recovery margin is small, within the range of spans tested (5.2 inches to 11.0 inches). The recovery margin varies by a maximum of 0.010 with pylon span.

3. A larger horizontal tail (area increased by 18.6 feet^2 and span increased by 20 inches) significantly increased the deep stall recovery margin. The available nose-down pitching moment coefficient at the critical angle of attack was increased due to the larger tail by from 0.049 to 0.065, depending on the flap and slat position.

4. The refan installation has no significant effect on elevator hinge moment characteristics.

5. In the normal flight regime, the refan engines cause a positive (airplane nose-up) increment in tail-off pitching moments and a slight increase in tail-off longitudinal stability.

6. In the normal flight regime, the refan engines do not significantly affect the DC-9 tail-on pitching moments. The refan engines apparently alter the downwash at the horizontal tail such that the change in tail contributions essentially offset the tail-off effects described above.

This test was made in conjunction with a high-speed test in the NASA ARC 11-foot facility. The purpose of the high speed test was to examine the effects of the larger nacelles and the nacelle-fuselage lateral spacing on cruise drag. The results are published in a separate report.

2.0 INTRODUCTION

On aircraft that have T-tails and aft-fuselage-mounted engines, such as the DC-9, the wing and nacelle wakes can blank out the horizontal tail at very high angles of attack - a condition commonly referred to as "deep stall". In this condition, which for the DC-9 is well beyond the normal stall, the blanketing effects of the wing and the nacelles and pylons reduce the effectiveness of the horizontal stabilizer and elevator. In addition, the elevator hinge moments are altered so that it is impossible to achieve full-down elevator with only the aerodynamic control tabs. Although this condition occurs well outside the normal operating envelope, it has been the position of the Douglas Aircraft Company to provide positive recovery capability and not rely on any mechanical devices which are intended to prevent entry into the deep stall. Also, a Douglas design requirement was that the aircraft must have pitch-down at the stall, and good stalling characteristics in general, so that there would be no natural tendency to enter a deep stall. Various design features insure that these goals are achieved on the DC-9. The horizontal tail was sized to provide positive recovery capability for all configurations and all centers of gravity within the established limits. An elevator power assist system provides emergency hydraulic power to the elevator to provide full-down elevator capability when the tabs become ineffective. Also, the underwing vortex-generating pylons, called "vortilons", insure pitch-down at the stall. The DC-9 pitching moment characteristics are typified in the sketch below.

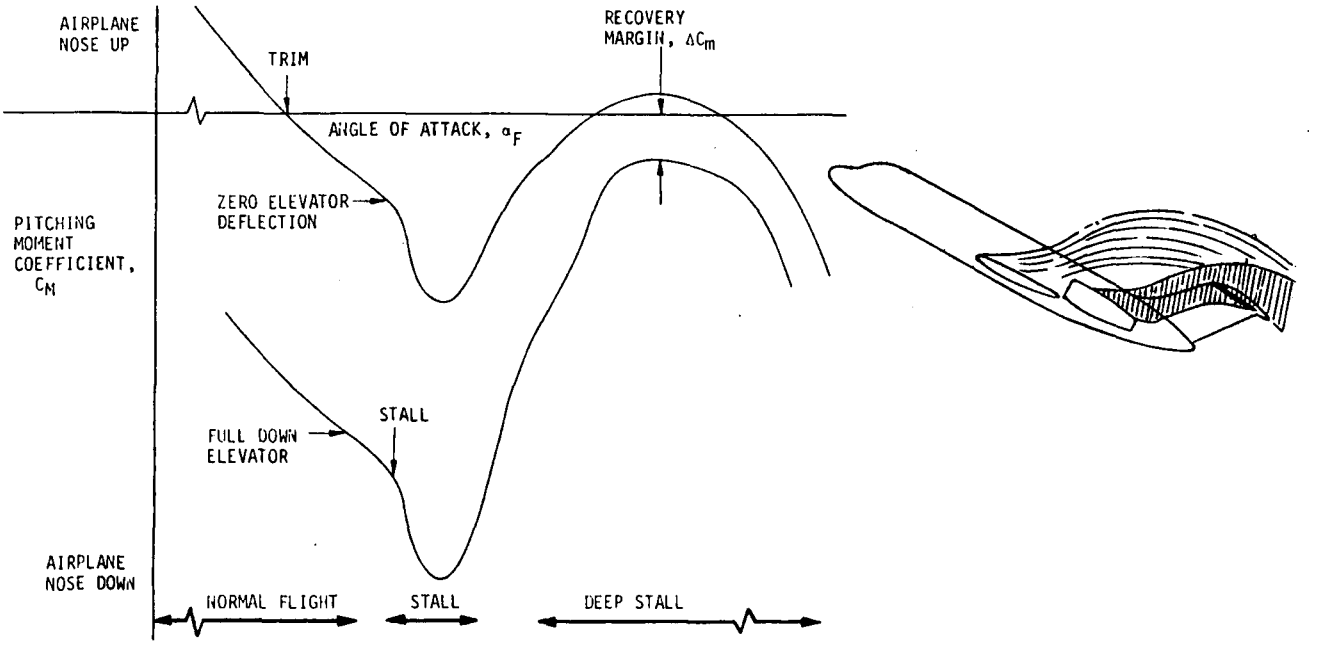

Installation of the larger-diameter refan nacelles on the existing pylons would increase the span of the nacelle-pylon combination, possibly creating a deep stall problem. Also, use of the present pylon would result in a larger thrust moment arm, due to the larger diameter of the refan nacelle, thus increasing engine-out minimum control speeds. In light of both the deep stall and engine-out aspects, it is desirable to install the refan engines in close to the fuselage with a pylon of shorter span. It was recognized that moving the nacelles in close to the fuselage could introduce an interference drag problem at cruise speeds. A high speed wind tunnel test at the NASA ARC 11-foot facility was conducted to investigate the effect of the larger nacelle and of the nacelle-fuselage lateral spacing on DC-9-30 cruise drag.

The results of the high speed test are reported in Reference 1. One of the conclusions arrived at from this test was that no drag penalty is experienced by shortening the pylon span from 16.7 inches (production) to 5.2 inches. A reduction in pylon span to 5.2 inches offsets the 11.5 inch increase in the refan nacelle diameter, keeping the outer nacelle line at the same lateral position as the existing nacelle. A cursory pylon accessibility study showed that this might be possible to build. However, more detailed studies showed that a minimum pylon span in the order of 7.5 to 8 inches was required.

A low-speed wind tunnel test was conducted during February and March 1973 in the NASA ARC 12-foot pressure wind tunnel to investigate the effects of the refan nacelle and various short-span pylons. Longitudinal characteristics were investigated with the primary areas of interest being the stall and deep stall regimes. The pertinent results are analyzed and discussed in this report.

3.0 SYMBOLS

$\bar{c}_e$	MAC of the elevator aft of the hinge line
CG	Center of gravity
C_{H_e}	Elevator hinge moment coefficient, $\frac{\text{hinge moment}}{q_o S_e \bar{c}_e}$, positive trailing edge down
C_L	Airplane lift coefficient, $\text{Lift}/q_o S_w$
C_m	Pitching moment coefficient, $\frac{\text{pitching moment}}{q_o S_w \bar{c}_w}$, positive airplane nose up
C_{m_A}	Total airplane pitching moment coefficient
$C_{m_{c/4}}$	C_m about the wing 1/4 MAC
ΔC_m	Incremental pitching moment coefficient
$C_{m_{C_L}}$	$\partial C_m / \partial C_L$
$C_{m_{\alpha_F}}$	$\partial C_m / \partial \alpha_F$
$\bar{c}_w$	MAC of the wing
EXT	Slats extended
H_{12D}	Production DC-9-30 horizontal tail
H_{14}	Enlarged horizontal tail - increased span of 20 inches and increased area of 18.6 feet^2 relative to H_{12D}
i_H	Horizontal stabilizer incidence, deg - positive trailing edge down
ℓ_i	Inlet length (from engine face)
L	Nozzle length
L/H	Nozzle length-to-height ratio
MAC	Mean aerodynamic chord
q_o	Freestream dynamic pressure, $0.7\ P_o M_o^2$
RET	Slats retracted
S_e	Elevator area aft of hinge line

S_W	Wing reference area
V_S	FAA approved stall speed
y	Pylon span
α_F	Fuselage angle of attack, deg
δ_e	Elevator deflection, deg - positive trailing edge down
δ_F	Flap deflection, deg

4.0 APPARATUS AND TESTS

4.1 MODEL DESCRIPTION

4.1.1 Basic Model

The model is a 9-percent scale representation of the DC-9-30 and is designated LB-155U. A three-view drawing of the DC-9-30 with the refan-engine nacelle is shown in Figure 1. The model was tested in the tail-on and tail-off configurations. The fuselage, wing, production empennage, and production nacelles and pylons have been previously tested in the Ames facility. A larger horizontal tail and the refan nacelles and pylons were fabricated specifically for this test program.

4.1.2 Nacelle Geometry

Because of the larger fan diameter of the JT8D refan engine (higher bypass ratio), the nacelle required to enclose the engine and accessories is also larger. The planform diameter is about 11.5 inches larger than the existing nacelle ($\approx$ 22 percent). The refan nacelle geometry has the following characteristics:

1. The inlet length from the engine face to the highlight is 43.0 inches,
2. The maximum nacelle diameter is 64.0 inches (plan view).
3. The nozzle L/H is 4.30 (L = 75.0 inches).
4. The overall nacelle length is 253.0 inches.
5. The nacelle is of long duct design very similar in overall appearance to the existing production nacelle.
6. The stang fairings required to enclose the thrust reverser operating linkage are simulated.
7. The afterbody boattail angle is 13.0 degrees.

A dimensional sketch of the refan nacelle compared to the baseline nacelle is presented in Figure 2.

4.1.3 Nacelle Installation Comparison

The installation of the refan nacelle compared to the production nacelle is shown in Figure 3. The pylon incidence is the same for both installations.

The inlet leading edge (highlight) is located 30 inches further forward and the nozzle is located 21.5 inches further aft. The model provided for three nacelle-pylon spacings which are described below:

1. P_{14}, y = 5.2 inches - stub pylon with the outside refan nacelle line coincident with the existing nacelle line. The planform span of the refan nacelle and pylon is the same as the production installation.

2. P_{19}, y = 7.5 inches - minimum spacing to provide adequate pylon accessibility without major redesign modifications to fuselage structure.

3. P_{15}, y = 11.0 inches - increased spacing to account for the possibility that future structural analyses dictate a larger pylon than 7.5 inches.

4.1.4 Horizontal Tail Geometry

Figure 4 shows the two horizontal tail configurations which were tested during the wind tunnel test (the basic production tail and an enlarged tail). The enlarged tail has an increased span of 20 inches and an increased area of 18.6 feet^2 relative to the basic DC-9-30 horizontal tail. The increased span is achieved by splitting the production horizontal tail at the centerline and adding a 20-inch span center section which extends the leading and trailing edge lines inboard. This increases the root chord from 132.7 inches to 136.6 inches and retains the tip chord of 46.8 inches. The quarter chord of the MAC for the modified tail is positioned at the same fuselage station as that of the basic tail. The new center section does not have elevators, so the elevator geometry is identical to the basic tail except for spanwise location.

4.2 TEST APPARATUS

4.2.1 Facility and Model Installation

The NASA Ames Research Center 12-foot pressure wind tunnel was used for this test program.

The model was installed with the DAC 6-5000-IB internal balance on the tandem two-strut support system as shown in Figure 5. This arrangement permitted the model to be pitched to angles of attack ranging from -10 degrees to 54 degrees. The extremely high angles of attack were necessary to investigate the deep stall regime.

4.2.2 Instrumentation

Six-component forces and moments were measured by the DAC-6-5000-IB internal balance and recorded through the Beckman 210 read-out equipment. The angle of attack of the model was set as indicated by a bubble pack installed within the aft fuselage of the model. Each bubble of the pack is oriented to a desired angle relative to the model fuselage reference plane and indicates the geometric angle of the model. The switch position which selects each bubble circuit provides a digital input to the Beckman for recording model angle of attack. Although the attitude of the model in pitch was set as indicated by the bubble pack, the angle of attack of the model for data reduction was determined from the output signal of a dangleometer. Two standard 60 degree dangleometers were installed within the model, one oriented to indicate angles of attack from -10 to +40 degrees, the other oriented to indicate angles of attack between zero and +54 degrees. The analog output of both dangleometers was recorded by the Beckman during the test.

Remote control systems were used to set the horizontal tail and elevator deflections. Positions of these surfaces were read out and recorded by the Beckman, and displayed at the control console by a digital interpretation of the voltage output from the position potentiometers.

Strain gages installed on the torque tubes of both the left and the right elevators sensed elevator hinge moments. The analog signal output of both gages was recorded through the Beckman, as well as displayed by a digital voltmeter at the control console.

4.3 TEST PROCEDURE AND DATA ACCURACY

The test was conducted at an elevated pressure level of 70 psia. The basic stability test runs (normal operating angle of attack range) were made at a nominal dynamic pressure of 270 psf, resulting in a Mach number of about 0.2, and a Reynolds number of 6.0 million per foot. When the model was pitched to the high angle of attack deep stall region, the dynamic pressure was reduced to a nominal 200 psf, resulting in a Mach number of about 0.18 and a Reynolds number of 5.2 million per foot. The Reynolds number was held constant within $\pm$ 100,000 during the test.

Selected pitch runs were repeated to ensure the validity of the data. The data repeatability was excellent throughout the test.

5.0 RESULTS AND DISCUSSION

5.1 DEEP STALL CHARACTERISTICS

5.1.1 Pitching Moments - Recovery Margins

The wind tunnel data of Figure 6 show pitching moment coefficient (about the wing MAC quarter chord) versus angle of attack, and compare the production DC-9-30 to the DC-9-30 with the refan nacelles and 7.5-inch pylons. These data are for a 50° flaps/slats extended configuration with the stabilizer set at -5 degrees (airplane nose up), and with the elevators at both 0 and +15 degrees (trailing edge down). The data, as shown, are not used directly to analyze deep stall recovery capability, but do illustrate the typical nature of the DC-9 longitudinal characteristics and the effects of the refan engine on those characteristics.

As can be seen in Figure 6, the aircraft exhibits strong positive stability (negative C_{m_α}) throughout the angle of attack range for normal flight. The model stalled at approximately 18 degrees angle of attack and displayed good pitch-down at the stall. Beyond the stall, at approximately 20 degrees angle of attack, the data show a reversal in pitching characteristics which reflect instability for a range of angles of attack up to 27 degrees for 0 degrees elevator or approximately 35 degrees for 15 degrees elevator deflection. This instability is caused by the tail entering first the wing wake and later the nacelle-pylon wake. At approximately 45 degrees angle of attack, positive stability is regained as the tail comes out of the bottom of the wake. The data also show the sharp reduction in elevator effectiveness that occurs in the deep stall area. The reduction in available nose-down pitch control due to the refan engine can be seen by comparing the data for the two configurations with full-down elevator (15°) at the minimum - C_m - margin angle of attack (approximately 40°). The data for other configurations tested vary in detail, but the trends are basically the same as those of Figure 6.

In order to evaluate deep stall recovery capability, the wind tunnel pitching moment data were adjusted to represent an aircraft trimmed at 1.3 V_S and the lift and drag data were used to correct the pitching moments to the aft center of gravity limit for the DC-9-30 (34.7% MAC). Figures 7 through 12 show the adjusted pitching moment coefficients versus angle of attack for various flap/slat combinations, pylon spans, and horizontal tails.

Figures 7 through 10 compare the baseline Series 30 to that with the refan nacelle and the 7.5 inch pylon for four flap/slat configurations. The data indicate that the refan nacelle-pylon reduced the recovery margins with full-down elevator by from 0.015 to 0.037 in pitching moment coefficient, depending upon flap/slat configuration. Figures 11 and 12 show the effects of the 5.2 and 11.0 inch pylons on the DC-9 with 50 degrees flaps. Comparison of these data to that for the 7.5 inch pylon indicates that the actual span of the pylon has little bearing on recovery margin. The effect of a larger horizontal tail is illustrated in Figure 10 which shows data for the refan configuration at 50° flaps with both the production and larger-than-production horizontal tails. A gain of 0.060 in recovery margin C_m is realized due to the larger tail.

A summary of the deep stall recovery margins plotted as a function of flap deflection is presented for all configurations tested in Figure 13. Examination of this figure shows the following:

1. Recovery margins are reduced somewhat with reduced flap setting. Slat position has a significant effect on the recovery margins, with gains of at least 0.15 due to slat retraction.

2. The refan installation, relative to the production installation, reduces the deep stall recovery margin by 0.015 to 0.037 in pitching moment coefficient, depending on flap and slat position and pylon span.

3. The deep stall recovery margins for the refan installation are essentially independent of pylon span, showing a variation of only 0.010 in pitching moment coefficient for the range of spans tested.

4. The larger horizontal tail significantly increased the deep stall recovery margin, as indicated by a gain of 0.049 to 0.065 in recovery pitching moment coefficient, depending on flap deflection and slat position.

The deep stall recovery margins are shown as a function of center of gravity position in Figure 14. Based on the trends of these data, it is concluded that the present center of gravity range (5.9% to 34.7% MAC) and horizontal tail size are acceptable for the DC-9-30 with the refan installation in so far as deep stall considerations are concerned.

5.1.2 Elevator Hinge Moment Characteristics

Comparison of the elevator hinge moment coefficients for the DC-9-30 baseline and refan configurations are shown as a function of angle of attack in Figures 15 and 16. As can be seen, the hinge moments at full-down elevator become very large at high angles of attack for all configurations. Previous wind tunnel data, which also included testing of the elevator tab effectiveness, revealed that the elevator would tend to travel trailing-edge-up at very high angles of attack, even with full trailing-edge-up tab. Since full down elevator is required for positive recovery from critical deep stall conditions, an elevator power assist system is provided on all DC-9 aircraft.

The data in Figures 15 and 16 show essentially no difference in the elevator hinge moments for the two configurations up through 45 degrees angle of attack. The minor variations can be considered as normal wind tunnel data scatter, since no consistent trends are indicated. Above 45 degrees angle of attack, the general trend is for the refan configuration to have somewhat lower hinge moments, but again, no real consistency is indicated in the data. Based on these data, it appears that the present authority of the power assist system will be adequate for the refanned DC-9-30.

5.2 PRE-STALL LONGITUDINAL CHARACTERISTICS

The effects of the refan nacelles and 7.5 inch pylons on the DC-9-30 pitching moment characteristics for the normal operating envelope are shown in Figure 17. Tail-off data are presented for 0°/RET, 0°/EXT, 25°/EXT, and 50°/EXT flap/slat configurations. Tail-on data are shown for 0°/EXT and 50°/EXT, the only tail-on configurations tested with the elevator undeflected.

A comparison of the tail-off data reveals that the refan nacelle causes a positive (nose-up) shift in the pitching moment coefficient at all flap settings. The shift is on the order of 0.035 to 0.05 at the lower lift coefficients. The effect was expected since the nacelles and pylons on the DC-9, being in a region of high downwash, normally experience a negative angle of attack and a download. Since the download acts aft of the CG and the nacelles have some negative camber, they contribute a positive pitching moment to the tail-off airplane. The larger refan nacelles would therefore be expected to increase this nose-up effect. The tail-off data also generally show that the refan nacelle-pylons have a mild stabilizing effect. This too is caused by the increased size of the refan nacelle and aft location of the DC-9 engines.

The tail-on data in Figure 17 indicate that the shifts in the tail-on pitching moments at a constant lift coefficient due to the refan engine are less than indicated with the tail off. Also, the tail-on data show little effect of the refan nacelles on stability, in terms of $C_{m_{C_L}}$. These characteristics are due to the effects of refan engines on the downwash at the horizontal tail. The DC-9 nacelles and pylons reduce the downwash at the tail, and the larger refan engines increase this effect. This reduction in downwash produces a nose-down pitching moment increment which tends to offset the nose-up moment with the tail off.

The conclusion drawn from these data are that the aircraft's longitudinal flight characteristics in the normal flight regime will be essentially unchanged by the refan installation. Tail-off pitching moment characteristics and downwash data will have to be adjusted, as indicated.

6.0 CONCLUSIONS

The results of the low speed wind tunnel test to determine the impact of the refan engines on the DC-9-30 low speed stability and control characteristics lead to the following conclusions.

1. The refan installation has a small effect on the DC-9-30 deep stall recovery capability, reducing the recovery margin approximately 0.015 to 0.037 in pitching moment coefficient, depending on flap and slat position and pylon span. Deep stall characteristics with the refan installation and any pylon span within the range tested are acceptable with no additional design changes anticipated.

2. The effect of pylon span on deep stall recovery margin is small, within the range of spans tested (5.2 inches to 11.0 inches). The recovery margin varies by a maximum of 0.010 with pylon span.

3. A larger horizontal tail (area increased by 18.6 feet^2 and span increased by 20 inches) significantly increased the deep stall recovery margin. The available nose down pitching moment coefficient at the critical angle of attack was increased due to the larger tail by from 0.049 to 0.065, depending on the flap and slat position.

4. The refan installation has no significant effect on elevator hinge moment characteristics.

5. In the normal flight regime, the refan engines cause a positive (airplane nose-up) increment in tail-off pitching moments and a slight increase in tail-off longitudinal stability.

6. In the normal flight regime, the refan engines do not significantly affect the DC-9 tail-on pitching moments. The refan engines apparently alter the downwash at the horizontal tail such that the change in tail contributions essentially offset the tail-off effects described above.

7.0 REFERENCES

1. Donelson, J.E., et al: "The Effects on Cruise Drag of Installing Refan-Engine Nacelles on the McDonnell Douglas DC-9." NASA CR-121219, 1973.

8.0 FIGURES

FIGURE	TITLE
1	DC-9-30 with Refan Engine Installation
2	Nacelle Geometry
3	Nacelle Installation Comparison
4	Horizontal Tail Geometry
5	Wind Tunnel Model Installation
6	Effects of NASA Refan Engines on Pitching Moment Coefficient - C_m vs α_F CG = 25% MAC, δ_F = 50°/EXT, production and 7.5" pylon
7	Effects of NASA Refan Engines on Pitching Moment Coefficient - C_m vs α_F CG = 34.7% MAC, δ_F = 0°/RET, production and 7.5" pylon
8	Effects of NASA Refan Engines on Pitching Moment Coefficient - C_m vs α_F CG = 34.7% MAC, δ_F = 0°/EXT, production and 7.5" pylon
9	Effects of NASA Refan Engines on Pitching Moment Coefficient - C_m vs α_F CG = 34.7% MAC, δ_F = 25°/EXT, production and 7.5" pylon
10	Effects of NASA Refan Engines on Pitching Moment Coefficient - C_m vs α_F CG = 34.7% MAC, δ_F = 50°/EXT, production and 7.5" pylon, H_{12D} and H_{14}
11	Effects of NASA Refan Engines on Pitching Moment Coefficient - C_m vs α_F CG = 34.7% MAC, δ_F = 50°/EXT, production and 5.2" pylon
12	Effects of NASA Refan Engines on Pitching Moment Coefficient - C_m vs α_F CG = 34.7% MAC, δ_F = 50°/EXT, production and 11.0" pylon
13	Effects of NASA Refan Engine on Deep Stall Recovery Margin - ΔC_m vs δ_F
14	Effects of NASA Refan Engine on Deep Stall Recovery Margin - ΔC_m vs CG
15	Effects of NASA Refan Engine on Elevator Hinge Moment Coefficient - C_{H_e} vs α_F, δ_F = 0°/RET and 0°/EXT, production and 7.5" pylon
16	Effects of NASA Refan Engine on Elevator Hinge Moment Coefficient - C_{H_e} vs α_F, δ_F = 25°/EXT and 50°/EXT, production and 7.5" pylon
17	Effects of NASA Refan Engines on Pitching Moment Characteristics C_L vs $C_{m_{\bar{c}/4}}$

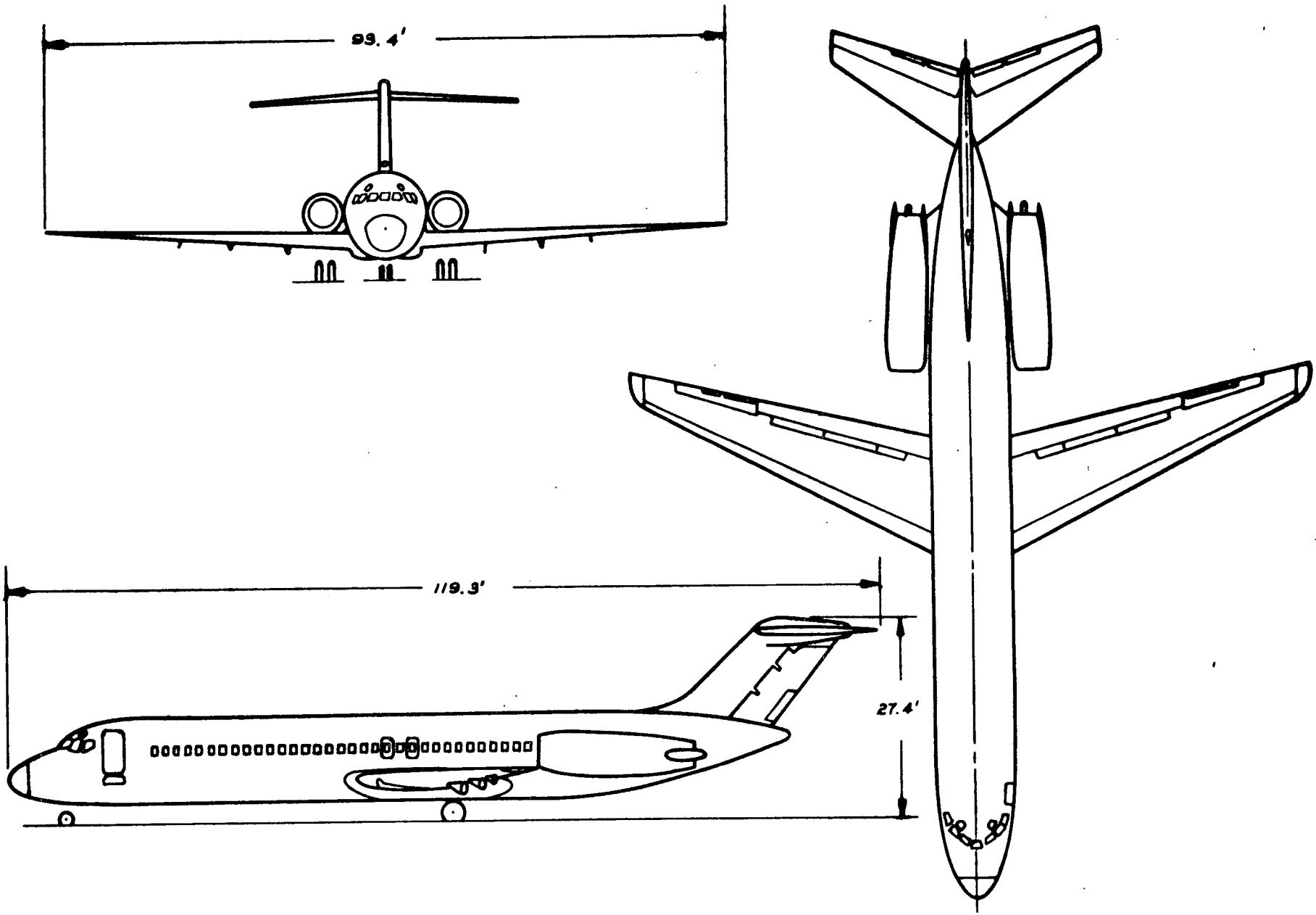

FIGURE 1 – DC-9-30 WITH REFAN ENGINE INSTALLATION

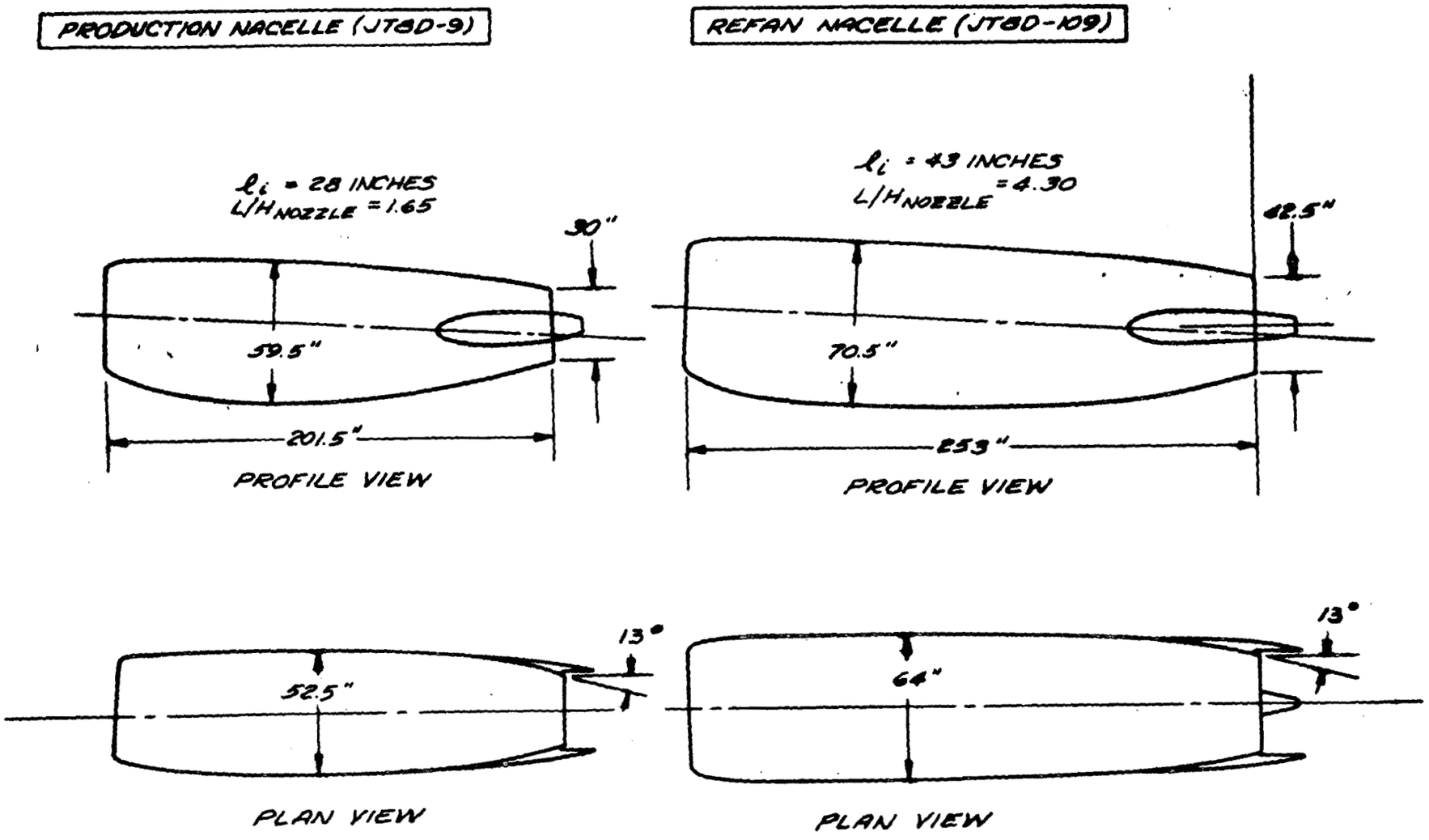

FIGURE 2 - NACELLE GEOMETRY

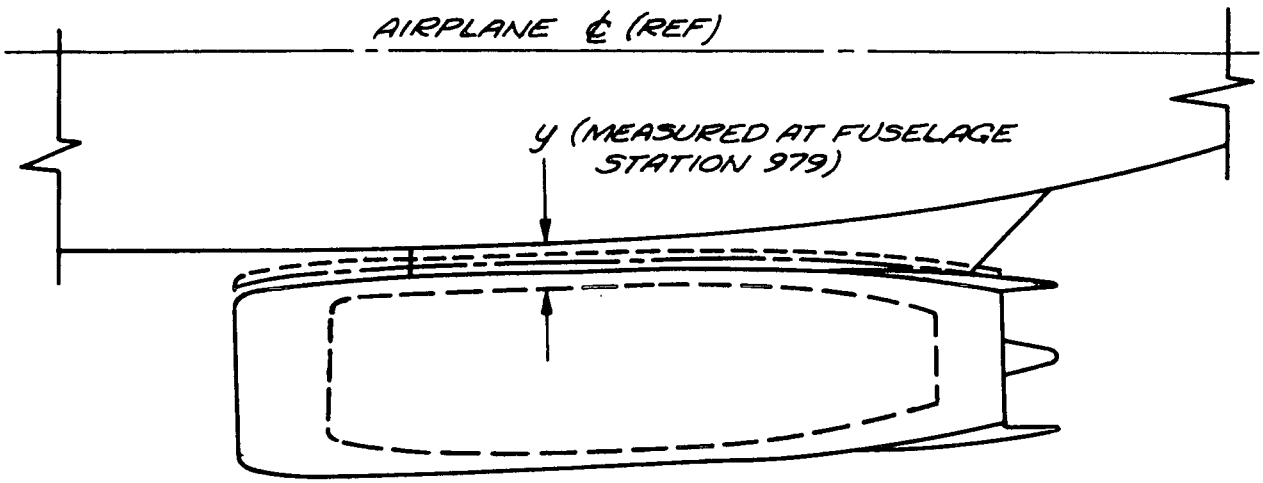

	NACELLE	PYLON SPAN y, INCHES
— — — —	PRODUCTION	16.7
————	REFAN	11.0
— - —	REFAN	7.5
- - - - - - - -	REFAN	5.2

PLAN VIEW

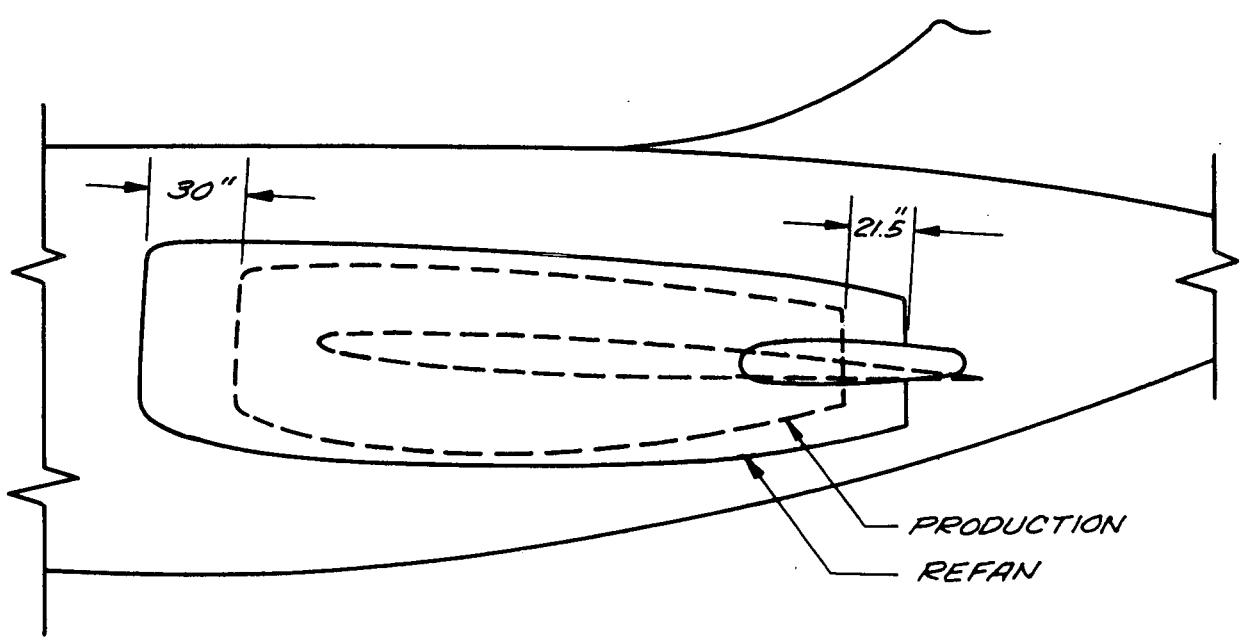

PROFILE VIEW

FIGURE 3 – NACELLE INSTALLATION COMPARISON

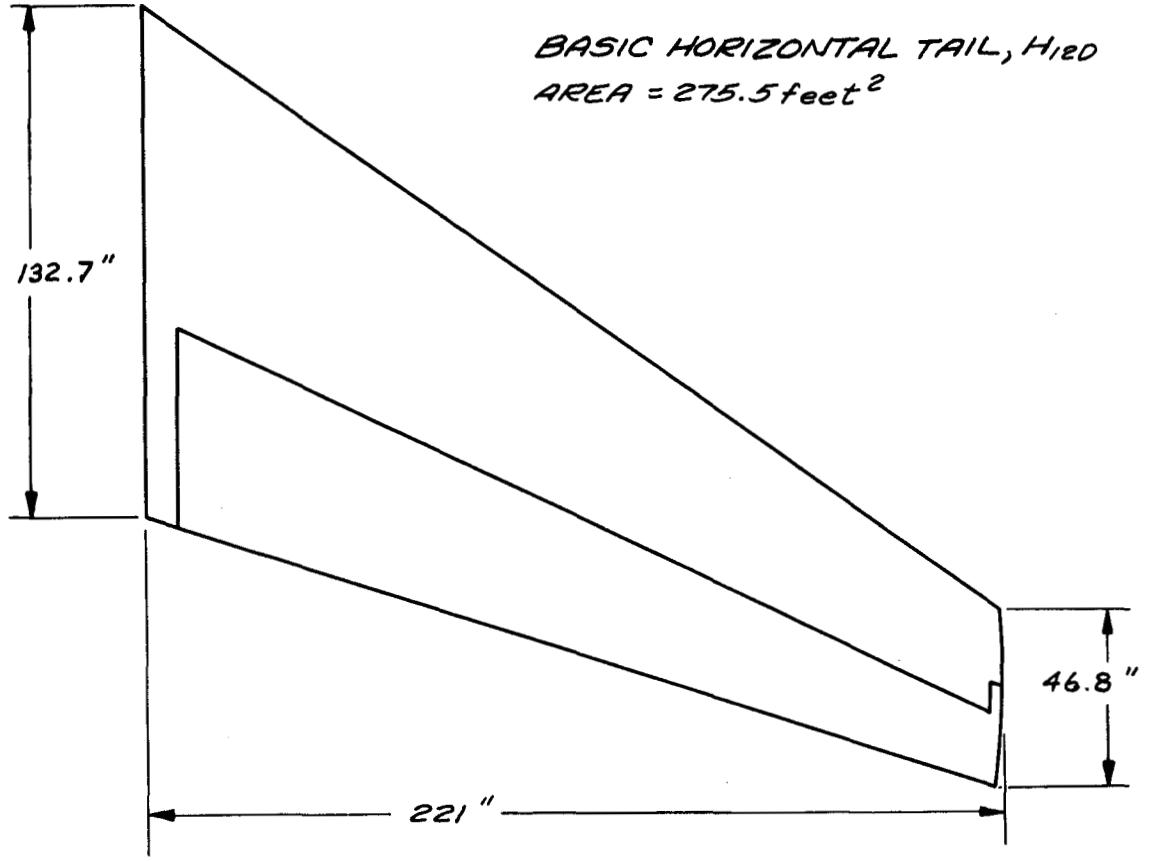

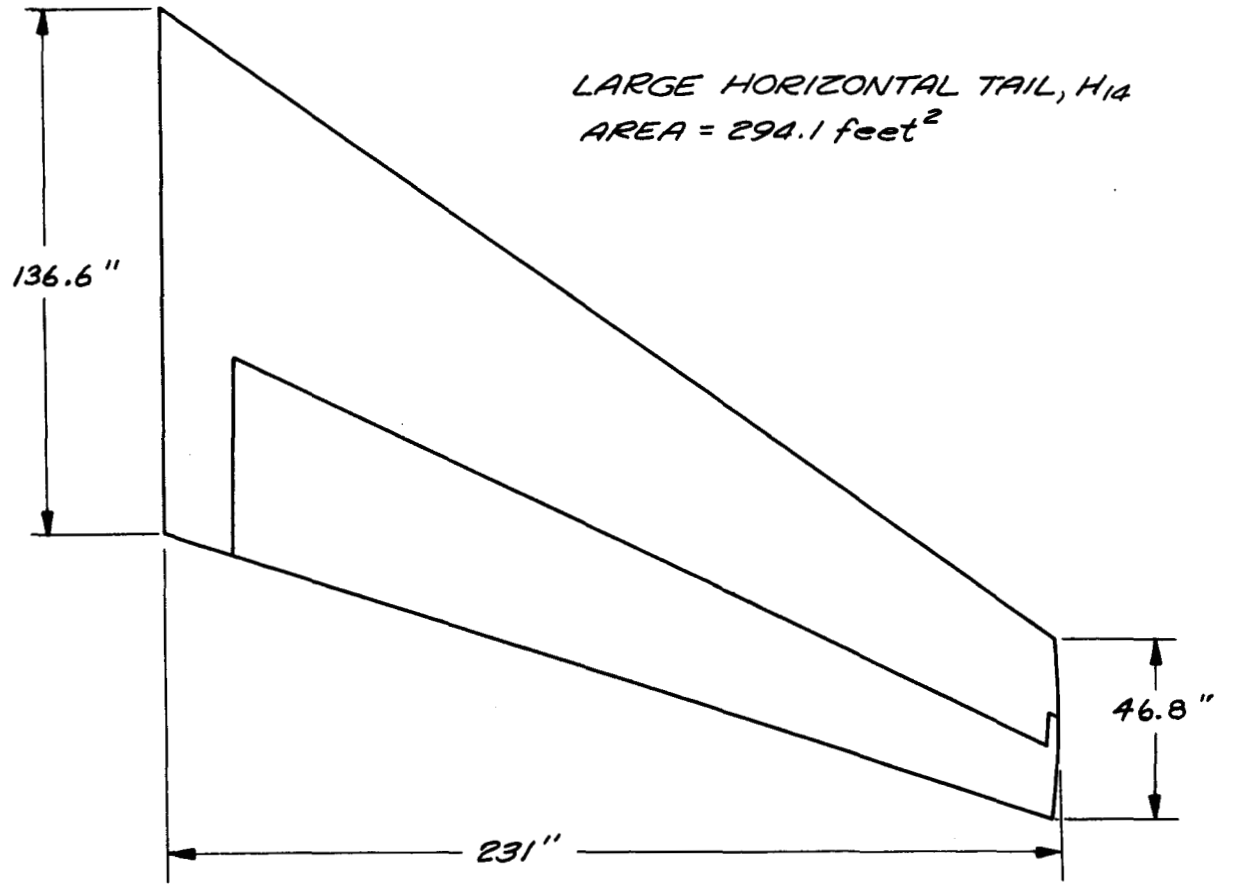

HORIZONTAL TAIL GEOMETRY
FIGURE 4

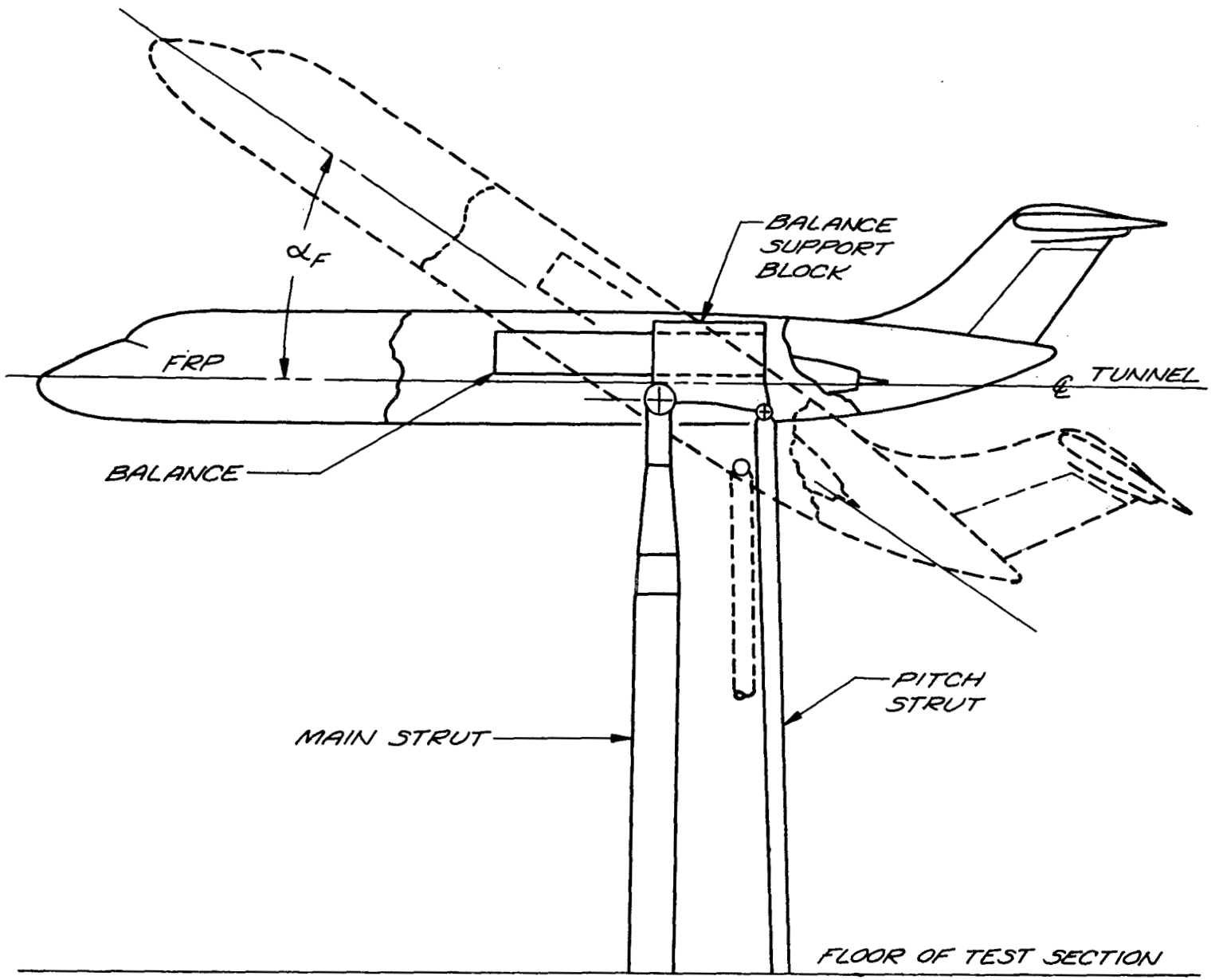

WIND TUNNEL MODEL INSTALLATION

FIGURE 5

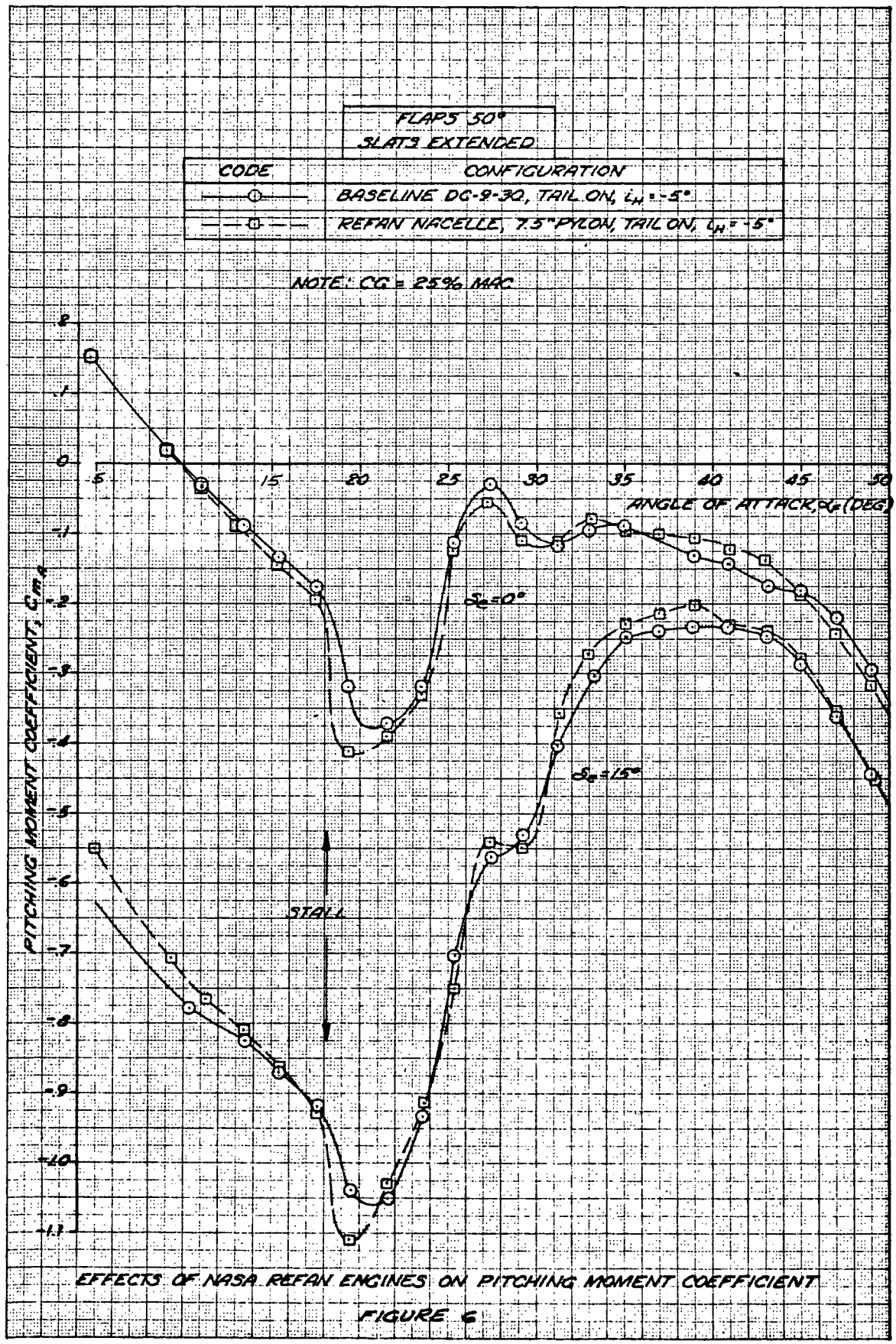

EFFECTS OF NASA REFAN ENGINES ON PITCHING MOMENT COEFFICIENT

FIGURE 6

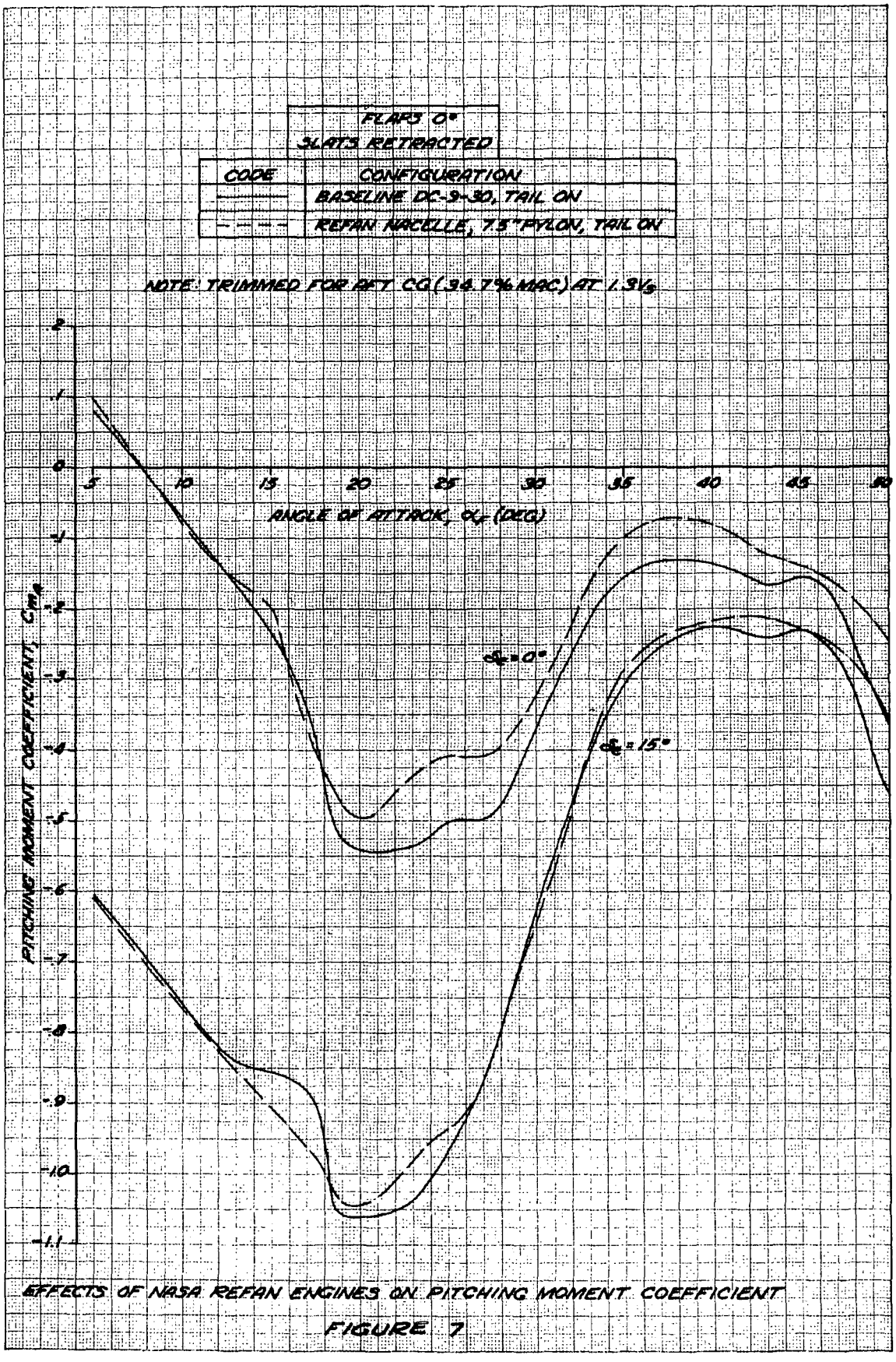

EFFECTS OF NASA REFAN ENGINES ON PITCHING MOMENT COEFFICIENT

FIGURE 7

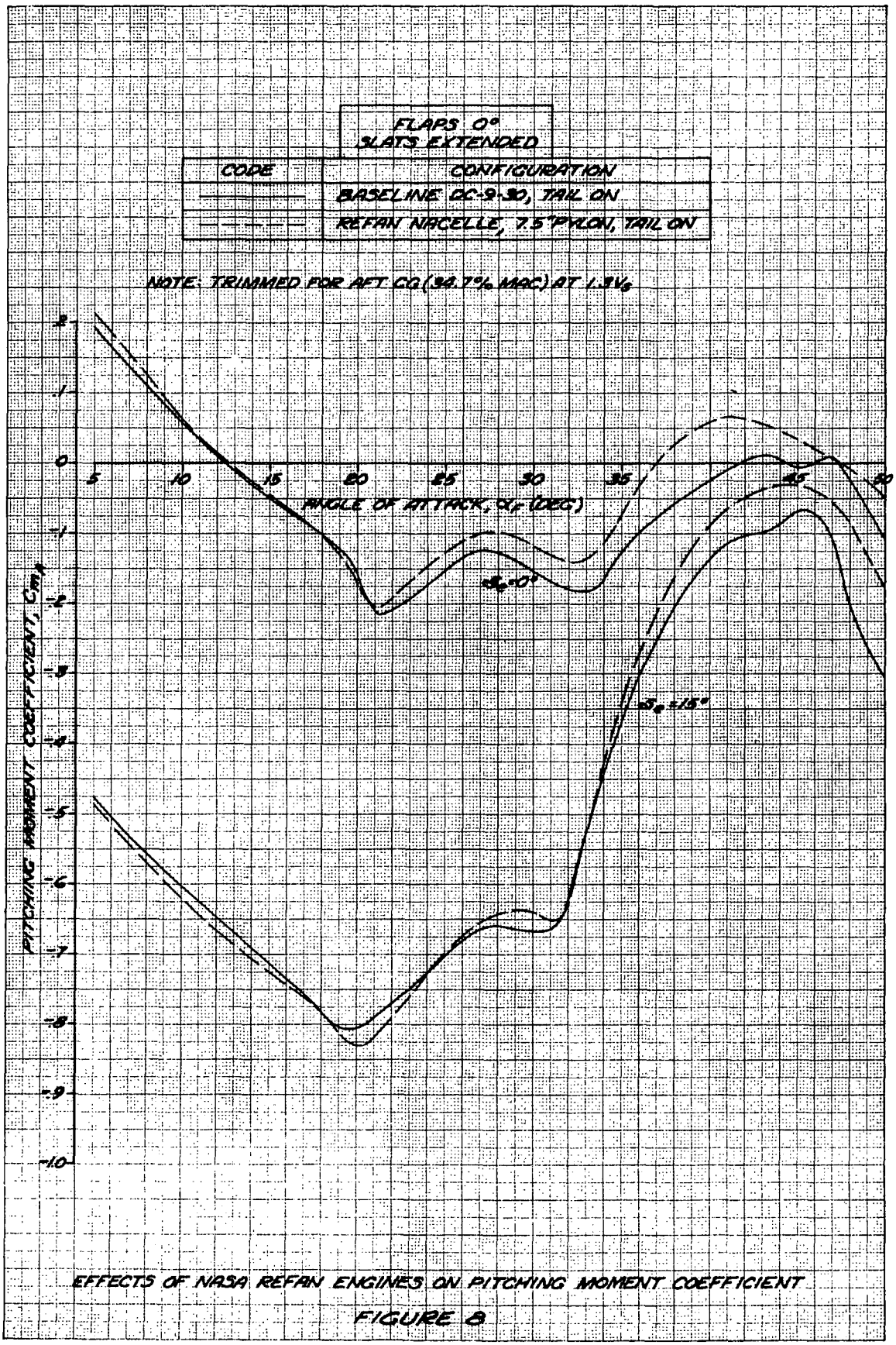

EFFECTS OF NASA REFAN ENGINES ON PITCHING MOMENT COEFFICIENT

FIGURE 8

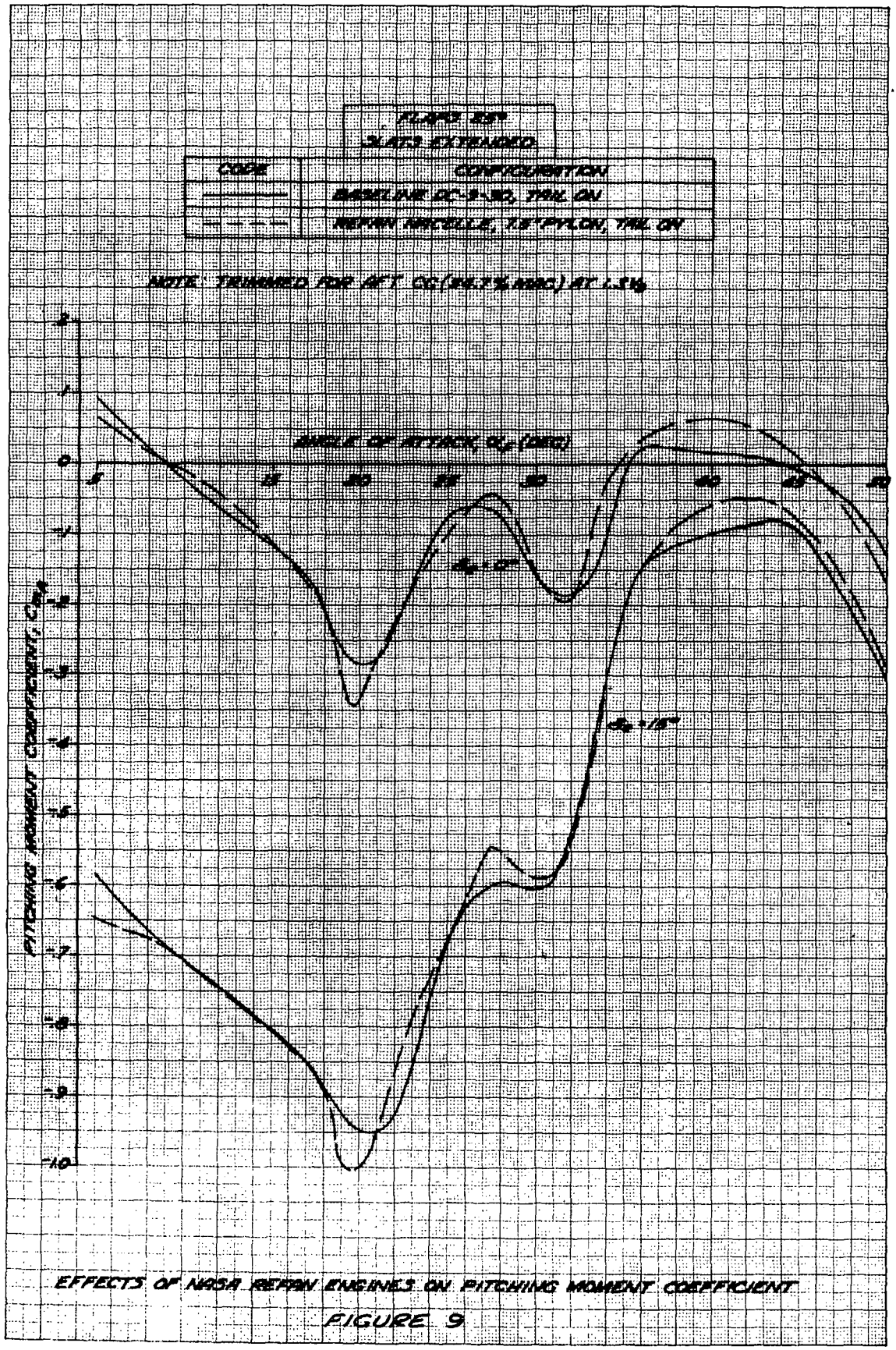

EFFECTS OF NASA REFAN ENGINES ON PITCHING MOMENT COEFFICIENT

FIGURE 9

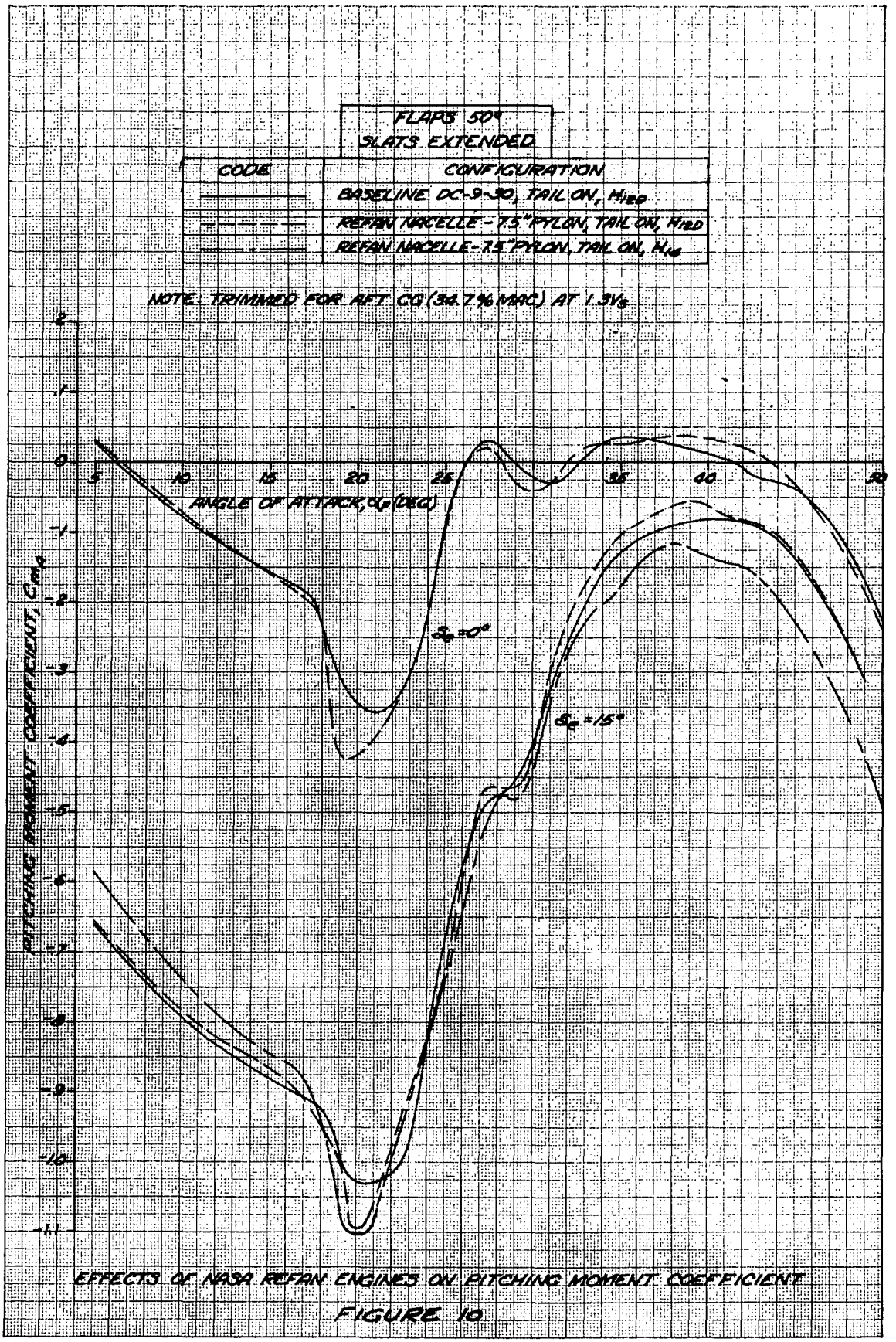

EFFECTS OF NASA REFAN ENGINES ON PITCHING MOMENT COEFFICIENT

FIGURE 10

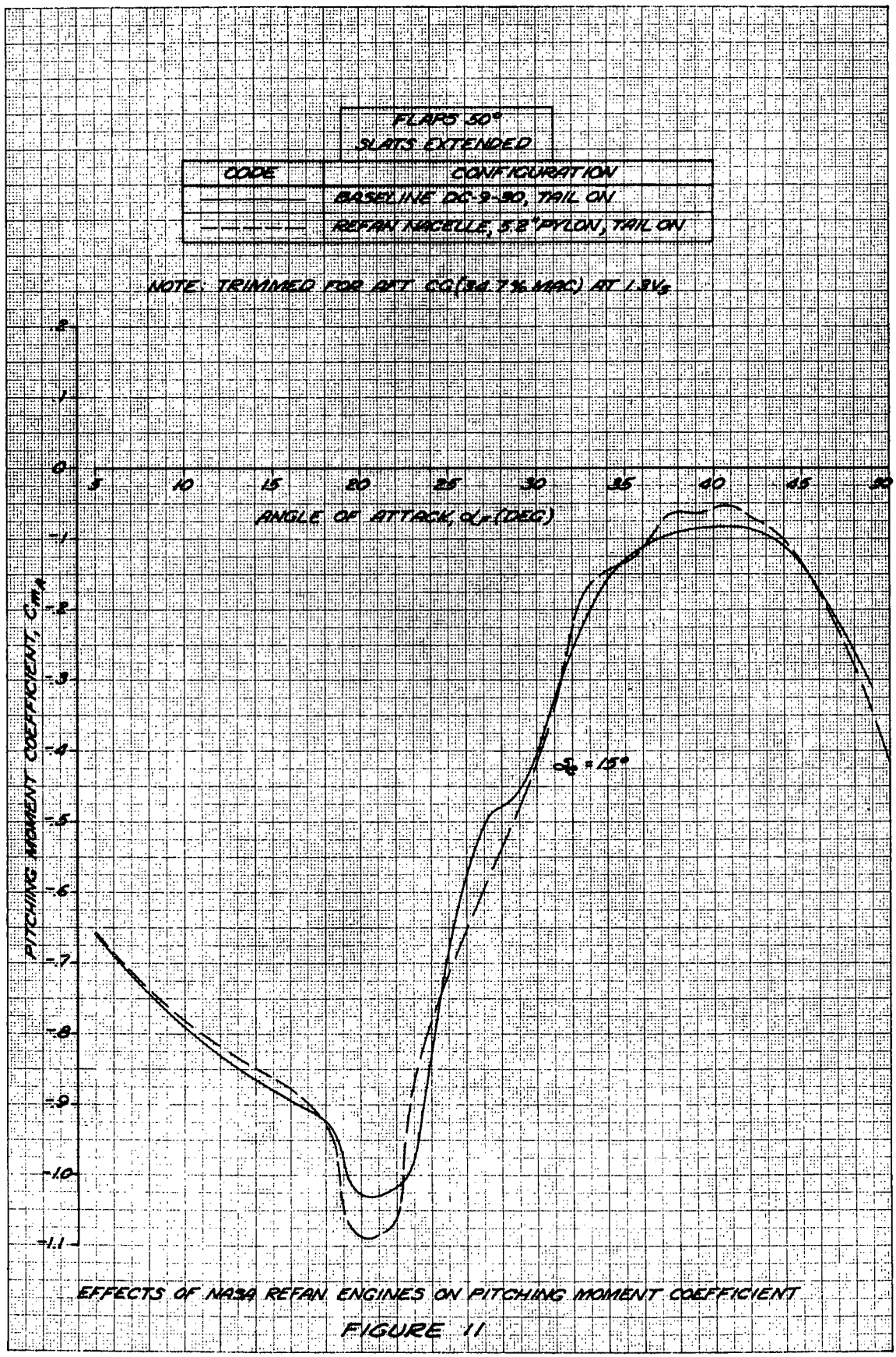

EFFECTS OF NA34 REFAN ENGINES ON PITCHING MOMENT COEFFICIENT

FIGURE 11

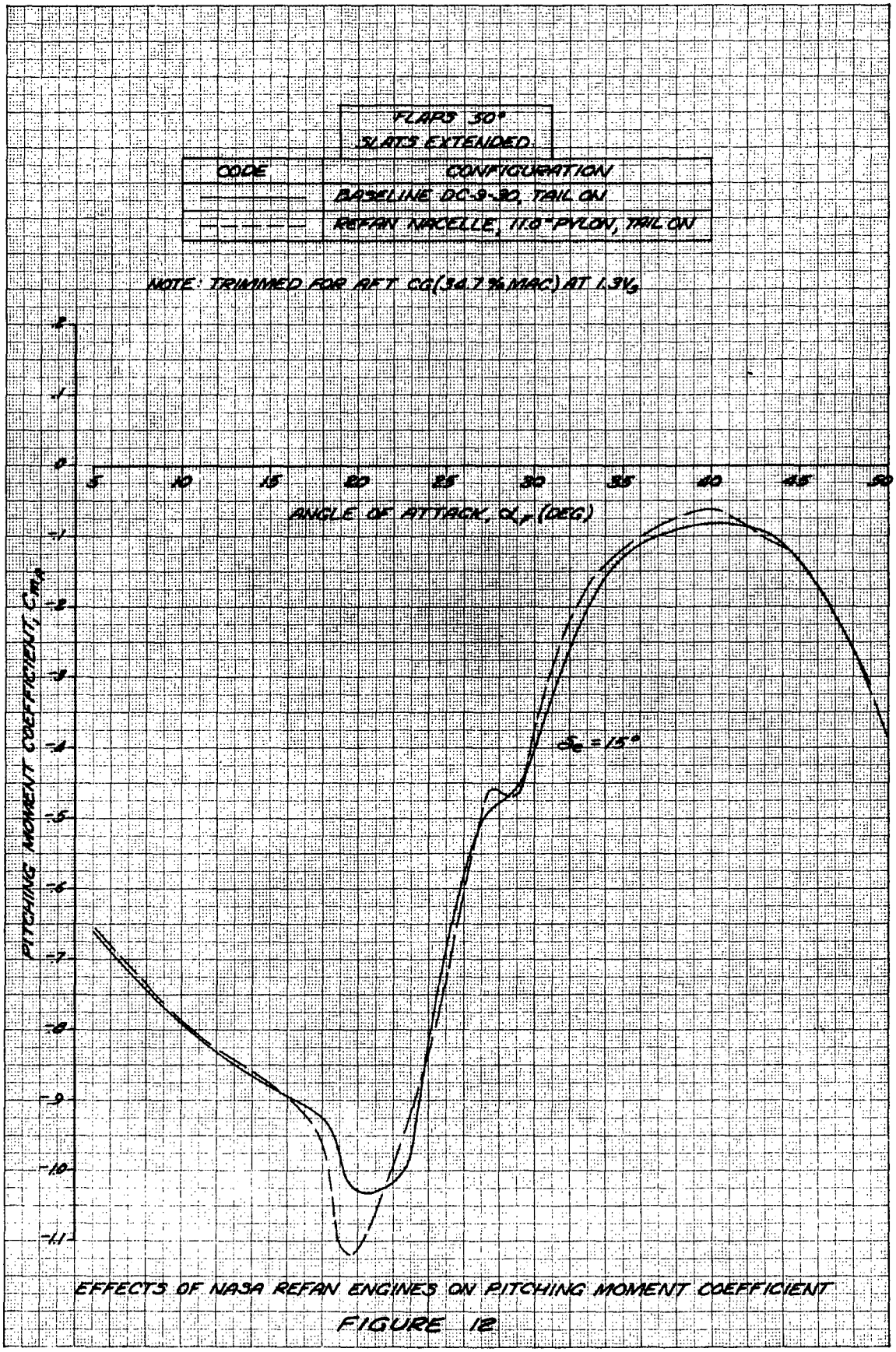

EFFECTS OF NASA REFAN ENGINES ON PITCHING MOMENT COEFFICIENT

FIGURE 12

SYMBOL	CONFIGURATION
○	BASELINE DC-9-30, BASIC TAIL, $\delta_e = 15°$
△	REFAN NACELLE-5.2" PYLON, BASIC TAIL, $\delta_e = 15°$
□	REFAN NACELLE-7.5" PYLON, BASIC TAIL, $\delta_e = 15°$
○	REFAN NACELLE-11.0" PYLON, BASIC TAIL, $\delta_e = 15°$
◇	REFAN NACELLE-7.5" PYLON, LARGE TAIL, $\delta_e = 15°$

NOTE: 1. TRIMMED FOR AFT CG (34.7% MAC) AT 1.3 V_S
2. OPEN SYMBOLS – SLATS EXTENDED
CLOSED SYMBOLS – SLATS RETRACTED

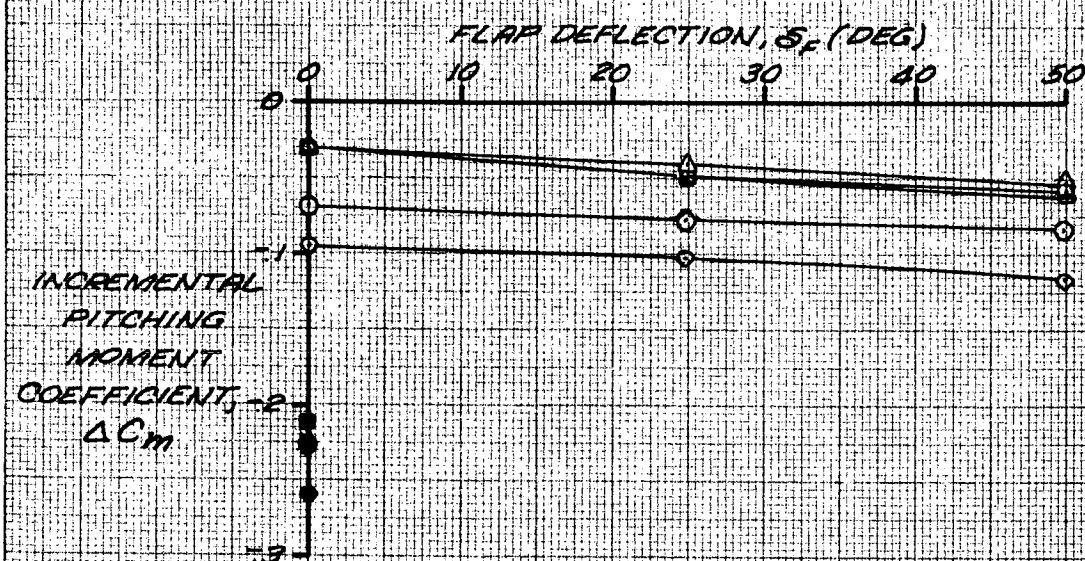

EFFECTS OF NASA REFAN ENGINES ON DEEP STALL RECOVERY MARGIN

FIGURE 13

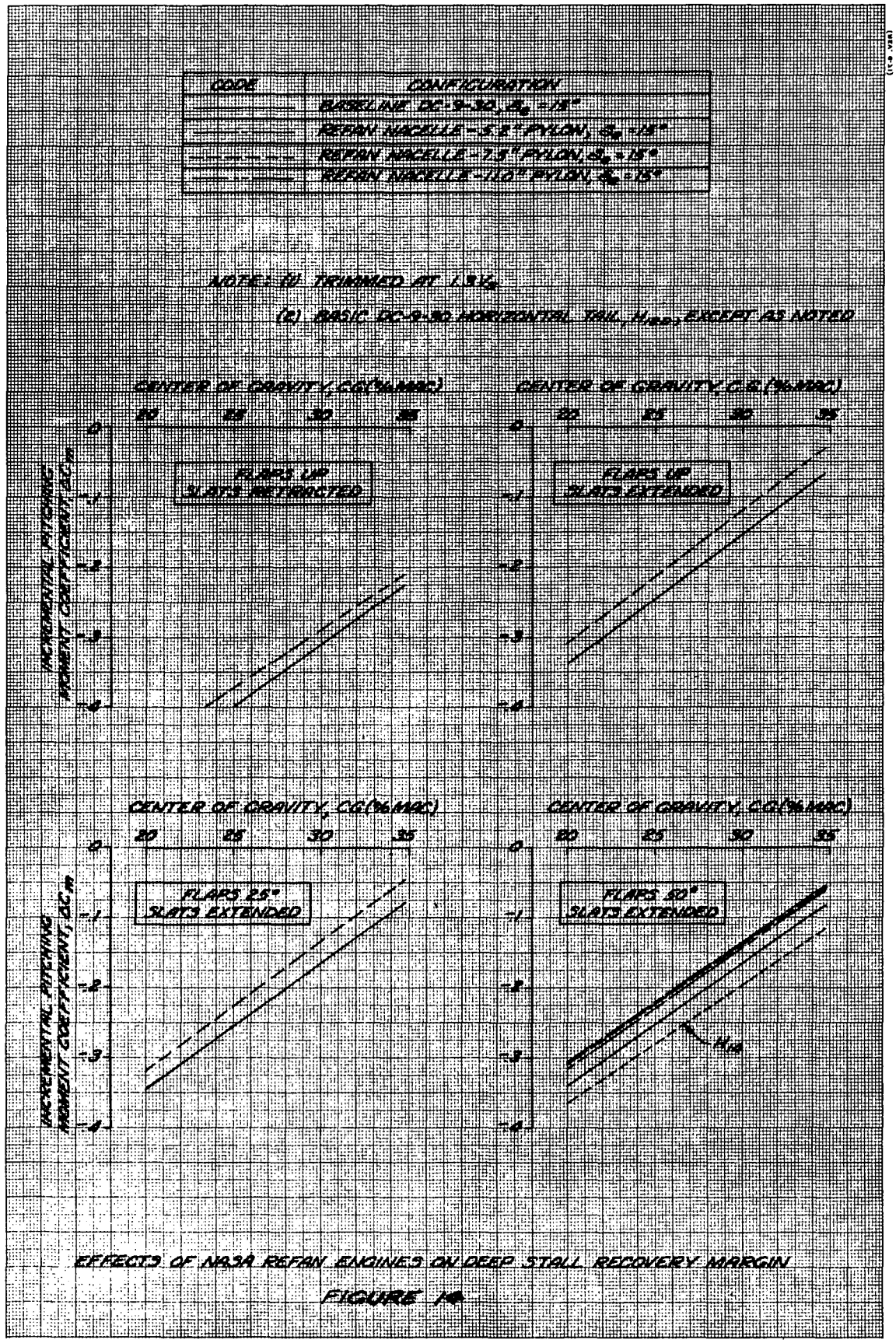

EFFECTS OF NASA REFAN ENGINES ON DEEP STALL RECOVERY MARGIN

FIGURE 14

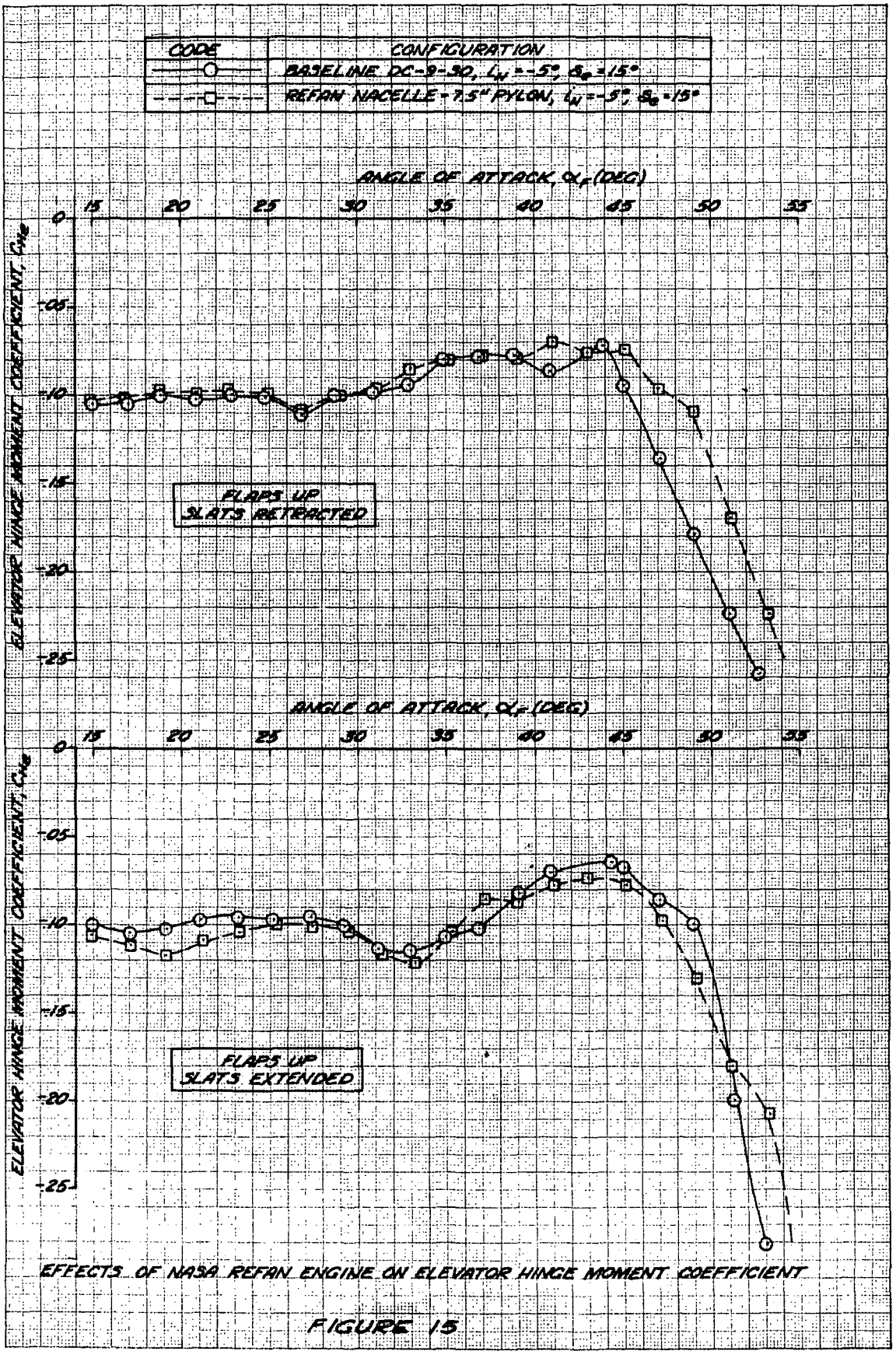

EFFECTS OF NASA REFAN ENGINE ON ELEVATOR HINGE MOMENT COEFFICIENT

FIGURE 15

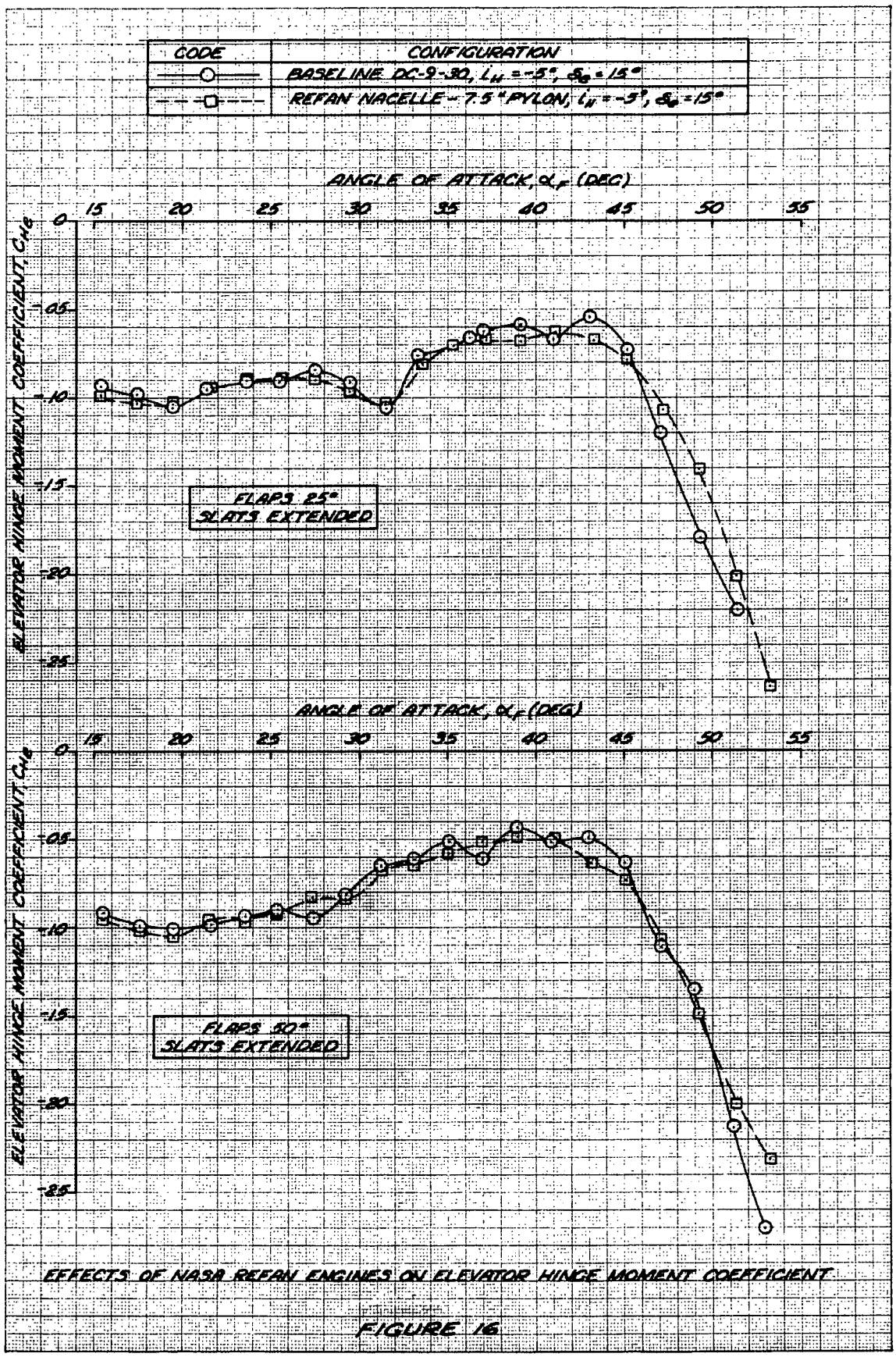

EFFECTS OF NASA REFAN ENGINES ON ELEVATOR HINGE MOMENT COEFFICIENT

FIGURE 16

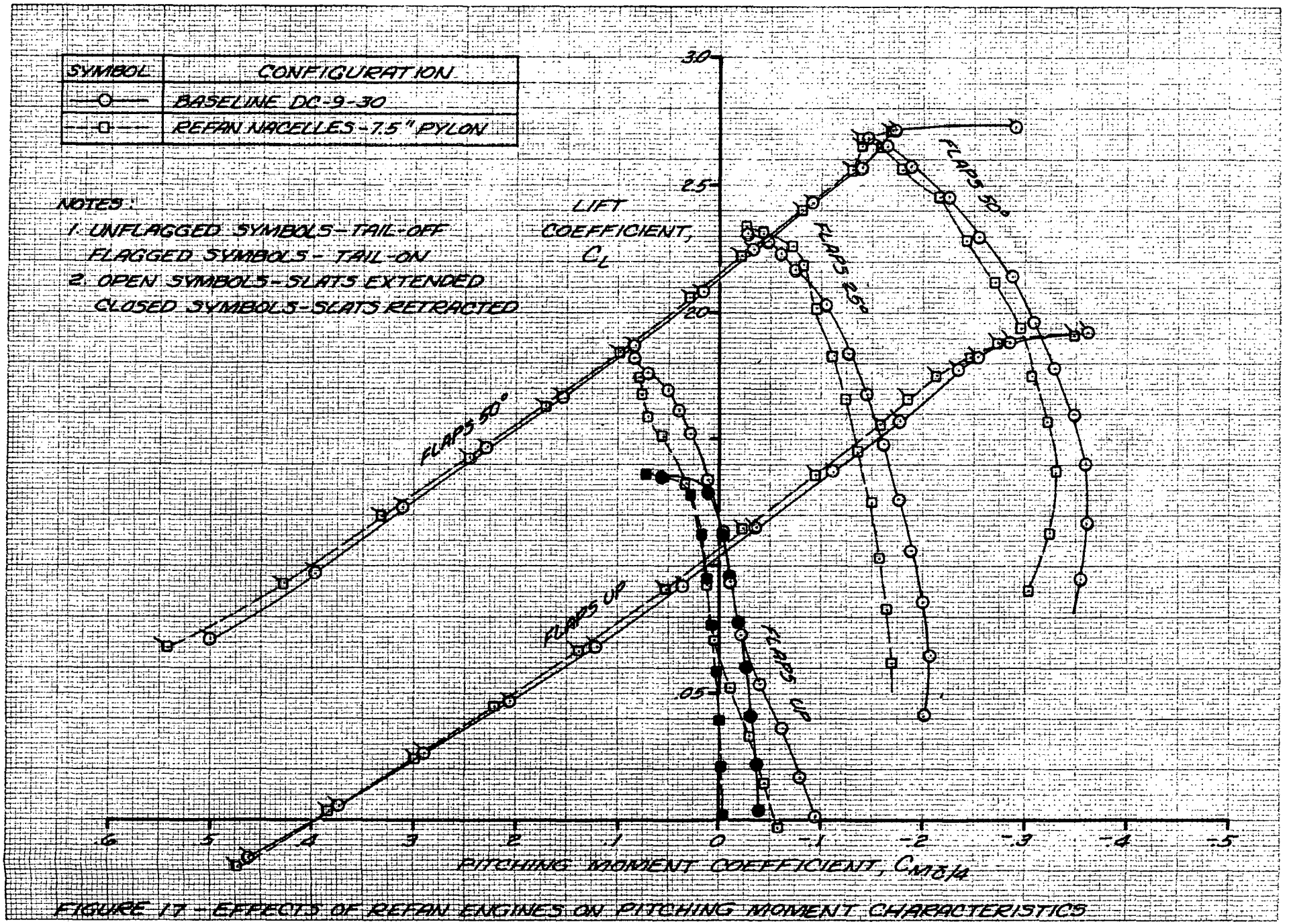

FIGURE 17 - EFFECTS OF REFAN ENGINES ON PITCHING MOMENT CHARACTERISTICS

REPORT DISTRIBUTION LIST

Addressee			Number of Copies
1. NASA Lewis Research Center 21000 Brookpark Road Cleveland, OH 44135 Attention:			
	Report Control Office	MS: 5-5	1
	Library	MS: 60-3	2
	Dr. B. Lubarsky	MS: 3-3	1
	A. A. Medeiros	MS: 501-7	25
	F. O. Driscoll	MS: 500-206	1
	N. T. Musial	MS: 500-113	1
	M. A. Beheim	MS: 86-1	1
	D. N. Bowditch	MS: 86-1	1
	F. A. Wilcox	MS: 86-1	1
	D. C. Mikkelson	MS: 86-1	1
	W. L. Stewart	MS: 501-5	1
	R. W. Schroeder	MS: 501-5	1
2. NASA Scientific and Technical Information Facility Attention: Acquisitions Branch P.O. Box 33 College Park, MD 20740			10
3. NASA Headquarters 600 Independence Avenue, S.W. Washington, DC 20546 Attention:			
	James J. Kramer (RJ)		1
	William H. Roudebush (RJ)		1
	Frederick P. Povinelli (RJ)		5
	Harry W. Johnson (RL)		1
	Kenneth E. Hodge (RO)		1
4. Environmental Protection Agency 8th Floor 1835 K. Street, N.W. Washington, DC 20460 Attention:			
	John Schettino		1
	William Sperry		1
5. Federal Aviation Administration 800 Independence Avenue, S.W. Washington, DC 20591 Attention:			
	Robert J. Koenig (Code ARD-551)		1
	James F. Woodall (Code ARD-500)		1

Addressee	Number of Copies
6. Office of Environmental Quality 800 Independence Avenue, S.W. Washington, DC 20591 Attention:	
John O. Powers (Code AEQ-2)	1
Richard P. Skully (Code AEQ-1)	1
7. Department of Transportation 400 7th Street, S.W. Washington, DC 20590 Attention:	
Charles R. Foster	1
Bernard Maggin (Code TST-51)	1
8. NASA Langley Research Center Hampton, VA 23365 Attention:	
Harry T. Norton, Jr. MS: 249A	1
9. NASA Ames Research Center Moffett Field, CA 94035 Attention:	
Stuart Treon	5
10. NASA Flight Research Center P.O. Box 273 Edwards, CA 93523 Attention:	
Donald Bellman Room 2106	1
11. United Air Lines SFO EG San Francisco International Airport San Francisco, CA 94128 Attention:	
L. C. Ellis	1
R. A. Gustafson	1
12. American Airlines 633 Third Avenue New York, NY 10017 Attention:	
G. P. Sallee	1
13. The Boeing Company Commercial Airplane Group P.O. Box 3707 Seattle, WA 98124 Attention:	
K. P. Rice	1
G. J. Schott	1
L. J. Winslow	1

Addressee			Number of Copies
14.	Pratt & Whitney Aircraft 400 Main Street East Hartford, CT 06108 Attention:		
	G. M. McRae		1
	D. L. Motycka		1
	W. J. Usab		1
15.	The Boeing Company 3801 South Oliver Street Witchita, KS 67210 Attention:		
	Floyd Palmer		1
16.	Pratt & Whitney Aircraft Florida Research and Development Center West Palm Beach, FL 33402 Attention:		
	Craig Swavely		1
17.	Rohr Corporation P.O. Box 878 Chula Vista, CA 92012 Attention:		
	F. A. Nickols		1
	F. Hom		1
18.	General Electric Company Aircraft Engine Group - E198 Cincinnati, OH 45215 Attention:		
	John T. Kutney		1
19.	LTV Aerospace Corporation P.O. Box 6267 Dallas, TX 75222 Attention:		
	F. T. Esenwein		1
	Francis Isley		1
20.	McDonnell Douglas Corporation Box 516 St. Louis, MO 63166 Attention:		
	Carl F. Schueller	MS: 152, Bldg. 33	1
21.	General Dynamics Corporation P.O. Box 748 Fort Worth, TX 76101 Attention:		
	Dave Bergman	MD 2887	1
	Frank Thebiay		1

Addressee	Number of Copies
22. Grumman Aerospace Corporation Bethpage, Long Island New York 11714 Attention: Gene Miller, Dept. 420 - Plant 35	1
23. Lockheed California Company P.O. Box 551 Burbank, CA 91503 Attention: John Stroud Harry Drell Tom Sedgwick	 1 1 1
24. Lockheed Georgia Company Marietta, GA 30060 Attention: J. P. Hancock J. M. Saylor	 1 1
25. North American Rockwell 4300 East Fifth Avenue Columbus, OH Attention: L. W. Throndson	 1
26. AF Flight Dynamics Laboratory (FDMM) Wright-Patterson AFB, OH 45433 Attention: J. A. Laughrey	 1
27. Allison Division, GMC P.O. Box 894 Indianapolis, IN 46206 Attention: Von D. Baker	 1
28. North American Rockwell Los Angeles Division International Airport Los Angeles, CA 90009 Attention: Leonard Rose	 1